PCCP

Accepted Manuscript

This is an *Accepted Manuscript*, which has been through the Royal Society of Chemistry peer review process and has been accepted for publication.

Accepted Manuscripts are published online shortly after acceptance, before technical editing, formatting and proof reading. Using this free service, authors can make their results available to the community, in citable form, before we publish the edited article. We will replace this *Accepted Manuscript* with the edited and formatted *Advance Article* as soon as it is available.

You can find more information about *Accepted Manuscripts* in the **Information for Authors**.

Please note that technical editing may introduce minor changes to the text and/or graphics, which may alter content. The journal's standard **Terms & Conditions** and the **Ethical guidelines** still apply. In no event shall the Royal Society of Chemistry be held responsible for any errors or omissions in this *Accepted Manuscript* or any consequences arising from the use of any information it contains.

ARTICLE

Dynamics of Li₄Ti₅O₁₂/sulfone-based electrolyte interfaces in Lithium-ion batteries

Julien Demeaux,*[abe] Eric De Vito,[d] Matthieu Le Digabel,[ab]
Hervé Galiano,[ab] Bénédicte Claude-Montigny,[bc] and Daniel Lemordant[bc]

Binary mixtures of cyclic (TMS) or acyclic sulfones (MIS, EIS and EMS) with EMC or DMC have been used in electrolytes containing LiPF₆ (1M) in both Li₄Ti₅O₁₂/Li half-cells and Li₄₊ₓTi₅O₁₂/Li₄Ti₅O₁₂ symmetric cells; and compared with standard EC/EMC or EC/DMC mixtures. In half-cells, sulfone-based electrolytes cannot be satisfactorily cycled owing to the formation of a resistive layer at the lithium interface, which is not stable and generates species (RSO₂⁻, RSO₃⁻) able to migrate toward the titanate electrode interface. Potentiostatic and galvanostatic tests in Li₄Ti₅O₁₂/Li half-cells show that charge transfer resistance increases drastically when sulfones are used in the electrolyte composition. Moreover, cycleability and coulombic efficiency are low. Conversely, when symmetric Li₄₊ₓTi₅O₁₂/Li₄Ti₅O₁₂ cells are used, it is demonstrated that MIS- (methyl isopropyl sulfone) and TMS- (tetra methyl sulfone) based electrolytes exhibit reasonable electrochemical performances as compared to the EC/DMC or EC/EMC standard mixtures. Surface analysis by XPS of both the Li₄₊ₓTi₅O₁₂ (partially oxidized) and Li₇Ti₅O₁₂ (reduced) electrodes taken from symmetric cells reveals that sulfones do not participate in the formation of surface layers. Alkylcarbonates (EMC or DMC), used as co-solvents in sulfone-based binary electrolytes, ensure the formation of surface layers at the titanate interfaces. Therefore, EMC reduction at the two Li₄₊ₓTi₅O₁₂/electrolyte interfaces in symmetric cells leads to the formation of carbonates, ethers and mineral compounds such as ROCO₂Li and Li₂CO₃. Finally, huge amounts of LiF are detected at the titanate electrode surface, resulting in an increase in resistivity of symmetric cells and causes capacity losses.

Introduction

Energy is an essential resource for modern society, but recent growing concerns over limited fossil-fuel resources and pollution have introduced the need to use renewable energy at large scale. Lithium-ion batteries are seriously considered as a source of energy storage for future HEV and EVs, what means more power and energy densities.[1,2] One solution to increase the stored energy will be to associate a high voltage cathode like LiNiₓMn₂₋ₓO₄ with a low potential anode, which can incorporate both rapidly and easily lithium ions in their structure while maintaining good durability over time and electrochemical cycling.[3] In commercial Li-ion batteries made of graphitic carbon, lithium plating and dendrite formation may occur at high power rates, leading to the risk of internal short circuits. Lithium titanate spinel Li₄Ti₅O₁₂ is an alternative to graphite as a negative electrode material, which allows for reversible insertion of up to three lithium ions per formula unit at a potential of 1.5 V vs. Li/Li⁺ and a practical specific capacity of 160–175 mAh g⁻¹. As sulfones exhibit an uncommon anodic stability up to 5.5 V vs. Li/Li⁺,[4] they are thus promising compounds for high-potential applications even if they suffer from a poor cathodic stability toward Li or carbonaceous anodes.[4,5] To the best of our knowledge, sulfones such as TMS (Tetra Methyl Sulfone), EMS (Ethyl Methyl Sulfone), MIS (Methyl Isopropyl Sulfone) and EIS (Ethyl Isopropyl Sulfone) have never been tested as electrolyte components in the presence of the titanate electrode (LTO or Li₄Ti₅O₁₂). In order to investigate the stability of these compounds toward reduction, LTO/Li and Li₄₊ₓTi₅O₁₂/Li₄Ti₅O₁₂ symmetric test cells will be used to evaluate the behaviour of alkylsulfones at their interfaces during cycling.[6]

The electrolytes used for this purpose are binary mixtures of cyclic (TMS) or acyclic sulfones (EMS, MIS and EIS) with either EMC (Ethyl Methyl Carbonate) or DMC (Di Methyl Carbonate) in which LiPF₆ is dissolved at the concentration of 1 mol.L⁻¹. The addition of the alkylcarbonates to sulfones is aimed to reduce their high viscosity and hence to enhance the ionic conductivity. Cycling tests using LTO/Li or Li₄₊ₓTi₅O₁₂/Li₄Ti₅O₁₂ cells will be performed in order to evaluate the performances of the different electrolytes. The

passive layer formed at the electrode interfaces will be studied by electrochemical impedance spectroscopy (EIS), scanning electron microscopy (SEM) and X-ray photoelectron spectroscopy (XPS) analysis in order to link the surface chemistry to the cell performances.

Experimental
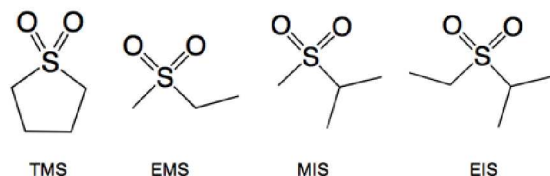
Fig. 1 Sulfones used in this study.

TMS (99.0%), EMS (98.0%), MIS (97.0%) and EIS (97.0%) were purchased from TCI (Tokyo Chemical Industry Co., LTD., Japan) and are presented in Figure 1. These solvents were distilled in order to reach purity over 99.9% (GC-MS, Agilent Technologies). EC, PC, EMC and DMC were obtained from Merck (battery grade) and used as received. Lithium hexafluorophosphate (LiPF$_6$, battery grade) was acquired from BASF. The binary electrolytes, listed in Table 1, were formulated in a glove box (< 0.1 ppm H$_2$O and O$_2$), dried below 10 ppm H$_2$O on molecular sieves (Merck) and the residual content in HF was certified to be less than 30 ppm by the Oesten's procedure.[7] All electrolytes, used in this study, are listed in Table 1.

A CDM210 conductimeter coupled with a CDC741T 2-pole cell (Radiometer Analytical) was utilized to measure ionic conductivities. The temperature control at 20.0°± 0.1°C was realized with a thermostatic bath ThermoHaacke C75P. The conductimeter was calibrated using standard solutions of known conductivities (0.10 and 0.01 mol.L^{-1} KCl in H$_2$O, Radiometer Analytical). Each conductivity was recorded when the stability was superior to 99% within 10 minutes. All the electrochemical tests were performed using a Versatile Multichannel Potentiostat VMP-3 (Bio-logic SA) piloted by an EC-Lab V10.23 interface.

Potentiostatic and galvanostatic experiments were carried out in coin-cells or HS-3E test cells (Hohsen Corp., Japan) with Li$_4$Ti$_5$O$_{12}$ (CEA-LITEN) and lithium (750 µm-thick, Alfa Aesar) as working and counter/reference electrodes respectively. The Li$_4$Ti$_5$O$_{12}$ composite positive electrode (1.54 cm^2 discs) is composed of 82/6/6/6 (wt. %) of respectively active material/carbon black (Super P, Timcal)/PVdF/Tenax fibers. All the electrochemical tests were performed in a climatic room at a controlled temperature of 20.0 ± 0.3°C, for cell configurations presented in Table 2. AC impedance spectroscopy was performed in the frequency range 1 MHz–10 mHz with an amplitude of 10 mV. The building of Li$_{4+x}$Ti$_5$O$_{12}$/Li$_4$Ti$_5$O$_{12}$ cells was already described.[6,8,9] Viledon/Celgard 2400 and Celgard 2400/Viledon/Celgard 2400

separator stacks were respectively used in LTO/lithium and symmetric cells. The volume of excess electrolyte used for these cells is displayed in Table 2. In the following, all potentials will be referred to the Li/Li$^+$ system.

Table 1 Electrolytes containing LiPF$_6$ (1M) used in this study. All compositions are given by weight.

Sulfone based electrolytes	Reference electrolytes
TMS/EMC (1/1)	EC/DMC (1/1)
TMS/DMC (1/1)	PC/DMC (1/1)
EMS/EMC (1/1)	EC/EMC (1/1)
EMS/DMC (1/1)	PC/EMC (1/1)
MIS/EMC (1/1)	
MIS/DMC (1/1)	
EIS/EMC (1/1)	
EIS/DMC (1/1)	

Table 2 Cell configuration and characteristics: separator stack, volume of electrolyte (V$_e$ in µL), working (WE), counter (CE) and reference (RE) electrodes.

	Separator stack	V$_e$ (µL)	WE[1]	CE	RE
Coin-cell Hohsen	Viledon/Celgard 2400	150	Li$_4$Ti$_5$O$_{12}$	Li[2]	
HS3E test cell	Viledon/Celgard 2400	300	Li$_4$Ti$_5$O$_{12}$	Li[1]	Li wire
Symmetric coin-cell	Celgard2400/Viledon/ Celgard 2400	150	Pre-lithiated Li$_{4+x}$Ti$_5$O$_{12}$	Li$_4$Ti$_5$O$_{12}$[1]	

[1] diameter, 14 mm; [2] diameter, 16 mm

XPS measurements are carried out with a SSI-SProbe spectrometer, using a focused monochromatised Al Kα radiation (hν = 1486.7 eV). Cells were disassembled in the glove box and electrodes samples were dried under vacuum for 48 hours at 50°C. The XPS spectrometer was connected through a transfer case filled with over pressure argon to avoid any sample exposure to moisture/air. Peaks were recorded with constant pass energy of 25 eV leading to an energy resolution around 730 meV. The pressure in the analysis chamber was around 10^{-9} mbar. Short acquisition time survey spectra were recorded before each normal experiment to search which elements were present at the electrode surface. The binding energy scale was calibrated from the hydrocarbon contamination using the C 1s peak at 285 eV. Core peaks were analysed using a non-linear Shirley-type background. The peak positions and areas were optimized by a weighted least squares fitting method using 70% Gaussian, 30% Lorentzian line shapes using CasaXPS® software. Quantification was performed on the basis of Scofield relative sensitivity factors.

Results and discussion

LTO/Li cells

POTENTIOSTATIC CYCLING The potential range of the Li$_4$Ti$_5$O$_{12}$/Li$_7$Ti$_5$O$_{12}$ system is around 1.5 V vs. LiC$_6$/C$_6$. Furthermore, EMS and EIS are known to be reduction sensitive at respectively 0.7 V vs. Li/Li$^+$ and 0.5 V vs. Li/Li$^+$.[10,11] Thus,

the potentiostatic cycling (CV) of $Li_4Ti_5O_{12}/Li$ cells is performed between 3.0 V vs. Li/Li^+ and 1.0 V vs. Li/Li^+ to exhibit eventual side reactions. As seen from the CV curves reported in Figures 2 and 3, no further reduction peaks, other than the one due to the Ti^{+III}/Ti^{+IV} system, are observed on the LTO electrode. In all voltammograms, the peak onset remains at a constant value of 1.55 V vs. Li/Li^+, independently of the electrolyte nature. Nevertheless, even at the low scan rate of 0.1 $mV.s^{-1}$, the difference in potential between the anodic and cathodic peaks (ΔE_1) at the 1st cycle increases and shifts from 278 to 617 mV when the EMC-electrolyte changes (Figure 2). The following order for increasing ΔE_1 is noticed:

EC/EMC (278 mV) < TMS/EMC (345 mV) < EMS/EMC (498 mV) < EIS/EMC (543 mV) < MIS/EMC (617 mV).
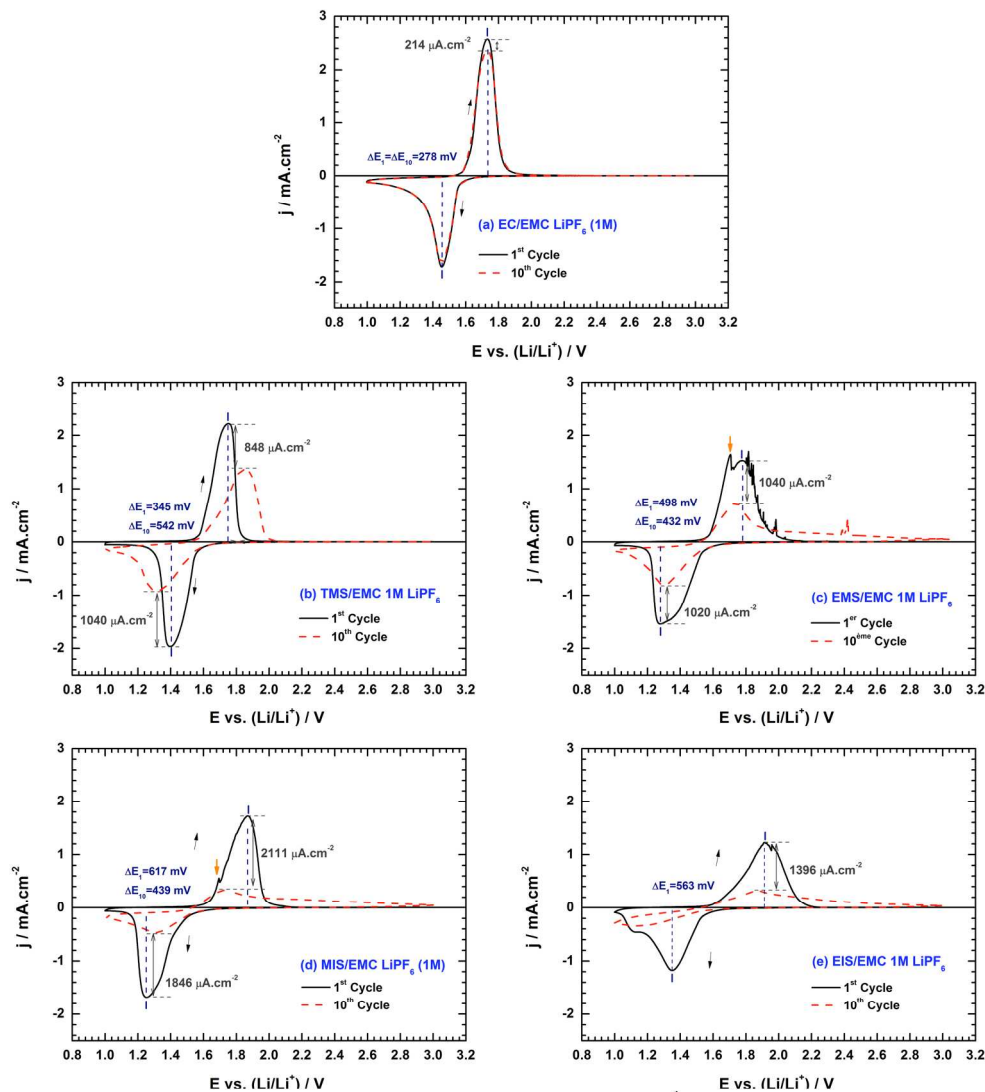
Fig. 2 CVs performed at the 1st and 10th cycle, on a $Li_4Ti_5O_{12}$ composite electrode at the rate of 0.1 mV s^{-1} versus a Li counter-electrode. *Sulfones are (b) TMS, (c) EMS, (d) MIS and (e) EIS in binary mixtures with EMC and LiPF$_6$ (1M) as salt.*

This means that the Ti^{+III}/Ti^{+IV} system is more electrochemically irreversible (or slow) in sulfones than in alkylcarbonates, in relation with their electrochemical properties of resulting electrode/electrolyte interfaces. For EMS/EMC, MIS/EMC and EIS/EMC (Figure 2, c to e), CVs indicate that a huge electrode polarization occurs at the 1st cycle. Moreover, at the 10th cycle, ΔE_{10} value shifts to a higher value for TMS/EMC and peak maximum values decrease for all sulfone-based electrolytes. This may be explained by the formation of a passivation layer at the electrode surfaces (Li or/and LTO), a phenomenon that could not be detected by CV

in the presence of the reference EC/EMC alkylcarbonate mixture. Additionally, an unidentified and uncharacteristic parasitic peak is observed at around 1.7 V on the CVs reported in Figure 2 (c and d), during the reverse scan which cannot be explained by the presence of an impurity in the electrolyte owing to its high purity (> 99.9%). In the same vein, small peaks, superposed to the main oxidation peak, are clearly visible between 1.7 V and 2.0 V for the EMS/EMC electrolyte and at 2.0 V for EIS/EMC.

CVs for the DMC-based electrolytes are represented in Figure 3. In both EMC and DMC binary mixtures with EMS,

MIS and EIS, the same parasitic peaks are noted. The most likely hypothesis is that, EMS, MIS and EIS are reduced at the lithium electrode and that their decomposition products are able to be re-oxidized at the LTO interface.[12] At the 10th cycle, reduction and re-oxidation processes of sulfones are responsible for a capacity estimated at 30 mAh.g^{-1}, which cannot be attributed to the Li$^+$ insertion/extraction in the LTO (Figure 4). On the contrary, no evolution of the CV curves is observed between the first and the tenth scan for the reference EC/EMC and EC/DMC electrolytes.
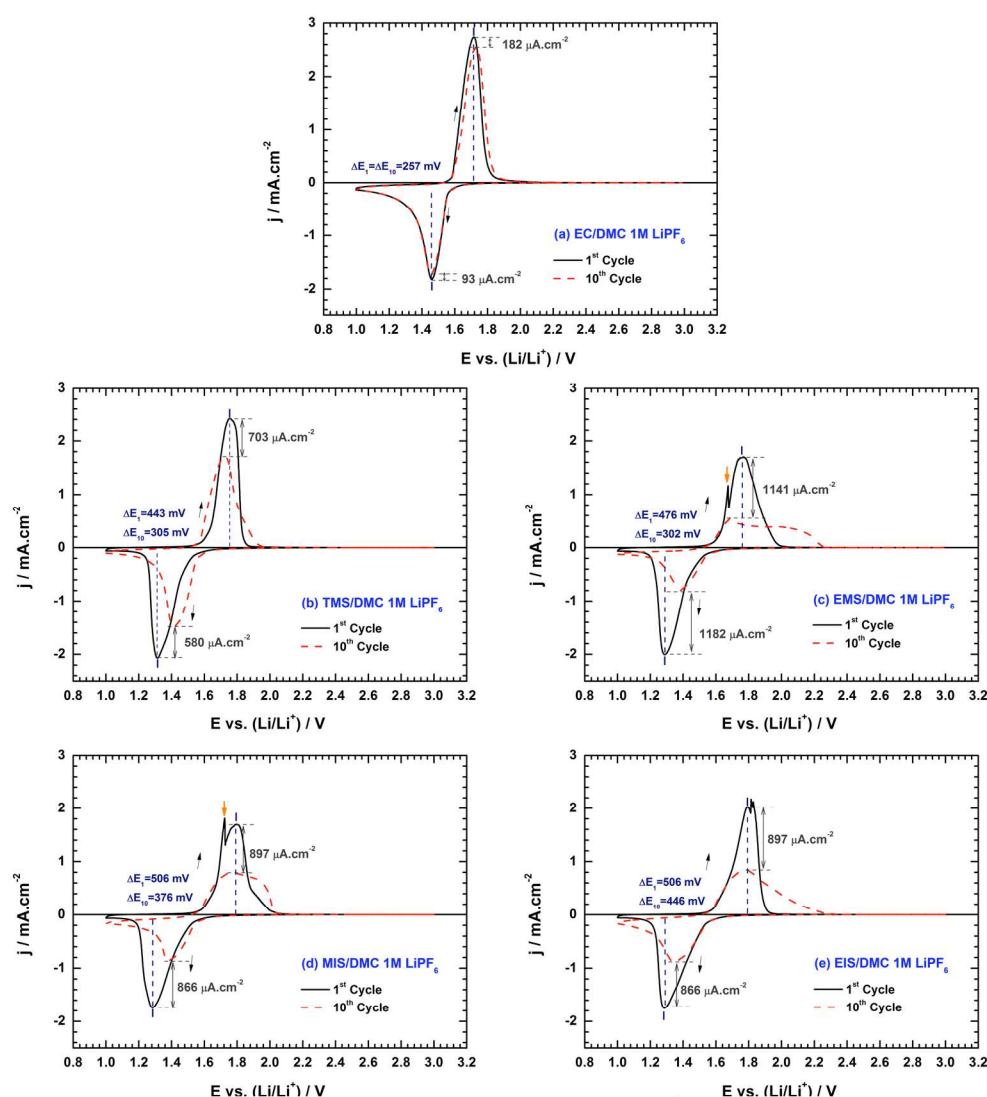
Fig. 3 CVs performed at the 1st and 10th cycle, on a Li$_4$Ti$_5$O$_{12}$ composite electrode at the rate of 0.1 mV s^{-1} versus a Li counter-electrode. Sulfones are (b) TMS, (c) EMS, (d) MIS and (e) EIS in binary mixtures with DMC and LiPF$_6$ (1M) as salt.

GALVANOSTATIC CYCLING In Figure 2b to e and Figure 3b to e, the drop in intensity of both the anodic and cathodic peaks is a striking feature that indicates an electrode capacity fading during the cycling. In order to verify this feature, a galvanostatic cycling procedure is performed on LTO/Li cells. The cycling procedure consists of applying alternatively slow (C/5+D/5, 35.0 mA g^{-1}) and fast (1C+1D, 175.2 mA g^{-1} or C/2+D/2, 87.6 mA g^{-1}) charge-discharge rates upon 100 cycles. Voltage profiles vs. specific capacity are displayed on the graphs reported in Figure 4 as a function of the cycle number (1st, 10th, 20th, 30th, 40th and 50th cycle) for the five EMC-based

electrolytes under consideration. Figure 5 shows the effect of cycling rates on normalized delithiation capacity (Q/Q$_0$), where Q$_0$ is the delithiation capacity at the first cycle. The Li$_4$Ti$_5$O$_{12}$/Li cells present very good cycleability with perfectly flat plateaus in the EC/EMC electrolyte (Figure 4a). Alkylcarbonate-based electrolytes are already known to behave as suitable electrolytes for LTO electrodes.[13] Indeed, after switching between slow and fast cycling, the capacity loss is only 2.7% for both EC/EMC and EC/DMC at the 100th cycle (Figure 5) and the mean coulumbic efficiency is almost 100.0% upon completion of the whole cycling period (Figure S1). On

the contrary, Li half-cells containing sulfone-based electrolytes with EMC or DMC as a co-solvent do not work properly because the specific capacity sharply decreases with cycle number (Figure 5). As seen from Figure 4 (b to e), the difference in potential between the delithiation and lithiation plateaus arises during the first 50 cycles indicating an increase

in resistivity of the coin-cells as confirmed by EIS measurements. After disassembling the coin-cells containing TMS, EMS, MIS and EIS, the lithium electrode exhibits an unusual reddish-yellow colour, which suggests the deposition of sulfureous derivatives, of which chemical nature has to be determined by XPS analysis.
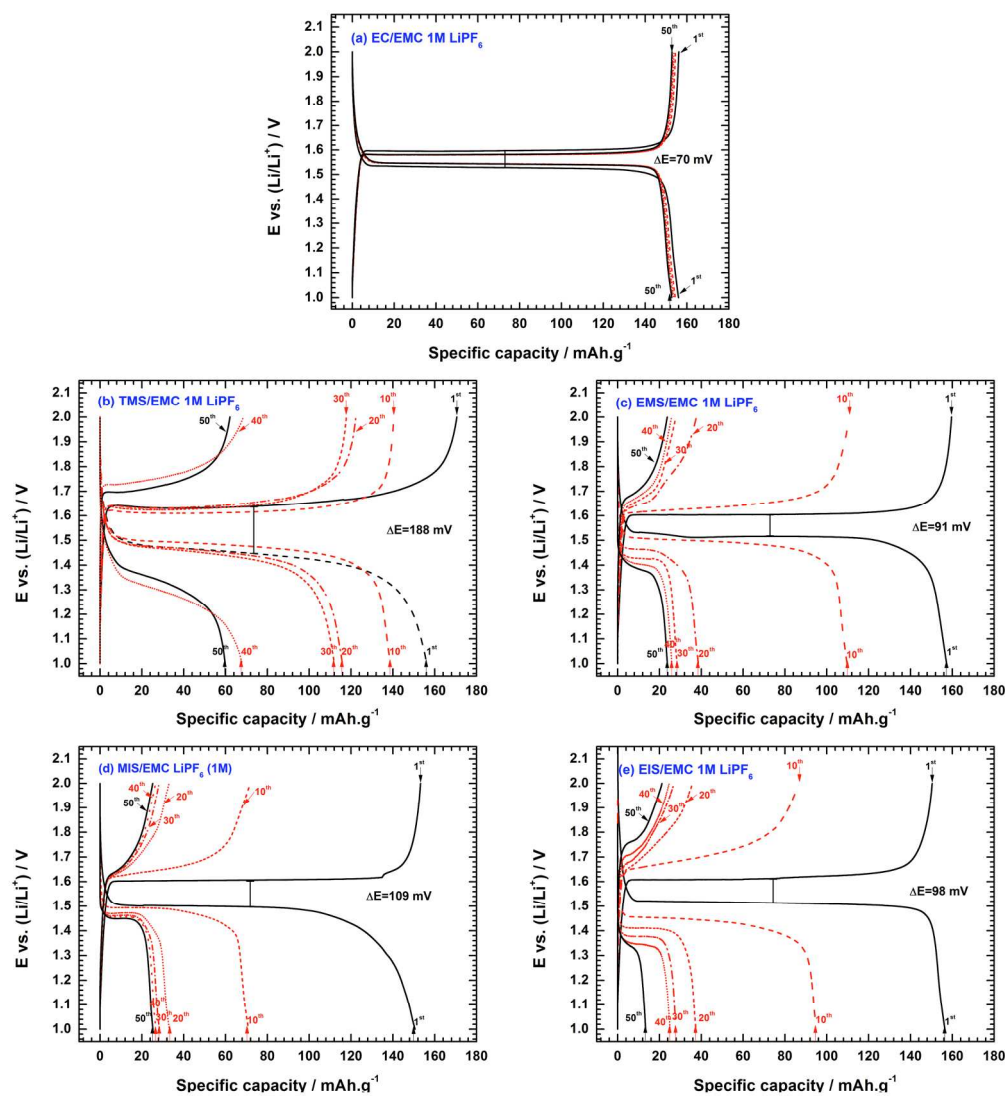
Fig. 4 Voltage profiles of LTO/Li half-cells cycled at charge-discharge rate of C/5+D/5 as a function of the cycle number at $20.0 \pm 0.3°C$. The $LiPF_6$ (1M) electrolytes are (a) EC/EMC, (b) TMS/EMC, (c) EMS/EMC, (d) MIS/EMC and (e) EIS/EMC.

For the EMC-based electrolytes, the capacity losses are similar: 86.6%, 88.6%, 90.8% and 88.6% for, respectively, the TMS, EMS, MIS and EIS based electrolytes after 100 cycles at the C/5+D/5 rate and very low capacities are observed at higher rates (1C+1D and C/2+D/2). In the same conditions, the mean coulombic efficiencies ($Ef = Q_{lithiation}/Q_{delithiation}$), are respectively 99.6%, 95.7%, 96.3% and 95.1% (Figures 5a and S1a). In the case of DMC-based electrolytes, capacity losses are reduced as compared to EMC but remain important: 27.2% ($Ef = 100\%$), 64.0% ($Ef = 81.4\%$), 76.6% ($Ef = 99.4\%$) and 26.7% ($Ef = 99.9\%$) for TMS, EMS, MIS and EIS respectively after 100 cycles (Figures 5b and S1b).

In conclusion, TMS is undoubtedly the best sulfone to be used in the $Li_4Ti_5O_{12}/Li$ cell configuration but remains inferior to its EC counterpart and higher cycleability is obtained when DMC is used instead EMC as co-solvent owing to its better stability LTO/Li cells. Moreover, when applying high current densities, TMS, EMS, MIS and EIS degradation products increase the coin-cell resistivities resulting in huge capacity losses. Therefore, LTO/Li cells cannot be correctly cycled when sulfones are blended with linear alkylcarbonates.
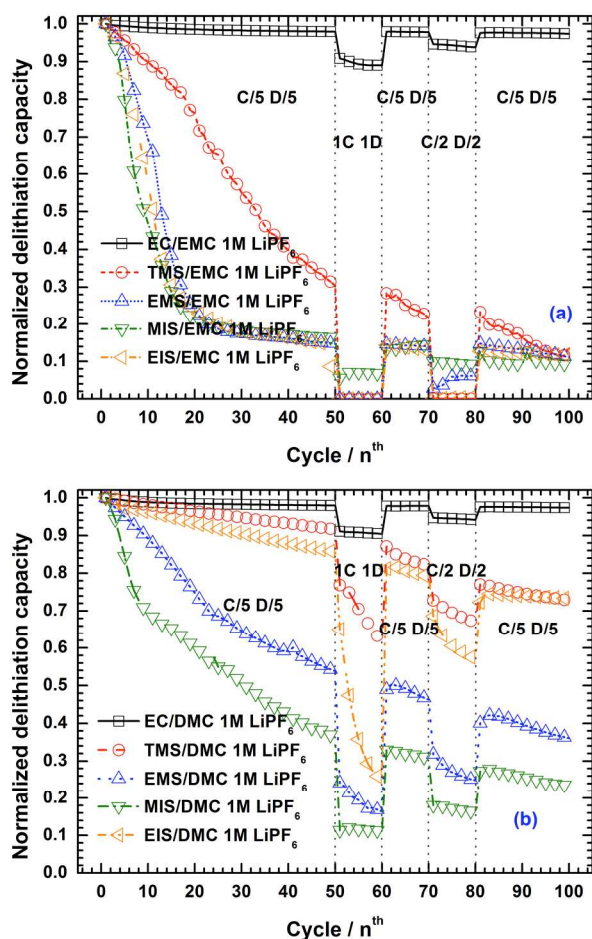
Fig. 5 Normalized delithiation capacity (Q/Q_0) versus cycling rate at $20.0 \pm 0.3°C$ of LTO/Li cells for the five (a) EMC-based and (b) DMC-based electrolytes.

IMPEDANCE MEASUREMENTS In order to quantify the increase in resistance when cycling LTO/Li coin-cells in the presence of sulfones, a three-electrode cell configuration was used to analyse both the LTO/electrolyte and the Li/electrolyte interfaces by EIS. For this purpose, in the case of EMC-based electrolytes, a Hohsen HS-3E test cell has been employed and cycled 100 times following the same procedure as previously used for the lithium coin-cells (Figure 5). This device was connected in a way that the counter electrode acts as a Li$^+$ reservoir. For impedance measurements, the cell is disconnected from the source of tension, to avoid any deposition of sulfone decomposition products on the reference electrode during cycling. The LTO/electrolyte and Li/electrolyte interface impedances were determined as a function of the frequency using a lithium wire as a reference electrode.
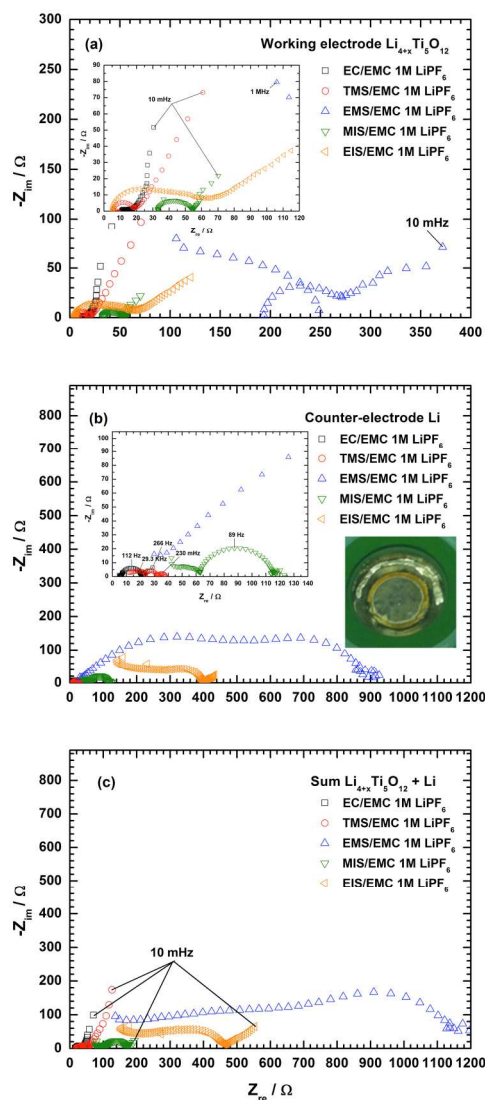
Fig. 6 EIS realized at OCV at the end of the 100th cycle. The contributions of the (a) LTO working electrode and (b) lithium counter-electrode on the (c) global impedance of the three-electrode cells are presented.

To check the influence of the cell configuration, all the EIS measurements on DMC-based electrolytes are performed with coin-cells. As shown in Figure 6, the impedance spectra of both the LTO and Li interfaces are composed of one or two semi-circles at high frequencies and a Warburg-type line at lower frequencies, which are characteristic of a passivation film layer at the electrode surface, a charge transfer impedance and diffusion in the active material.[14]
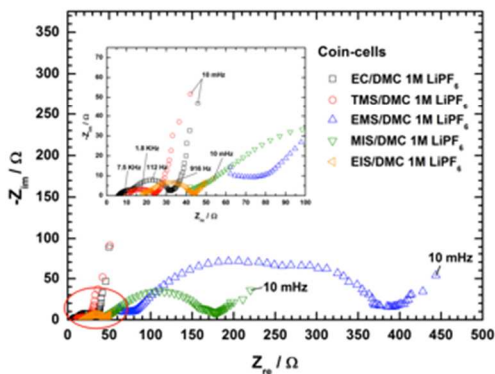
Fig. 7 Electrochemical impedance spectroscopy realized at open circuit potential on two-electrode LTO/Li half-cells using DMC-based electrolytes at the end of the 100th cycle.

All EMC/sulfone-based electrolytes exhibit a huge increase in resistivity compared to the reference EC/EMC electrolyte. This confirms the observations done in Figure 4. In particular, reduction reactions occurring at the Li/electrolyte interface lead to a larger increase in impedance than at the LTO/electrolyte interface (see Figure 6 a and b). At the same time, the surface aspect of the Li electrode is strongly modified: when de-assembling both the HS-3E and the coin-cells, reddish-yellow species are observed at its surface and on the separators in the case of sulfones mixed with linear carbonates. Coloured deposited species are the main cause of the growth in impedance of the Li-electrode (EIS reported in Figure 6 and Figure 7), which results in the half-cell failure.

Fig. 8 Voltage profiles (C/5+D/5) at 20.0 ± 0.3°C for (a) EC/EMC 1M LiPF$_6$, (b) TMS/EMC 1M LiPF$_6$, (c) EMC/EMC 1M LiPF$_6$, (d) MIS/EMC 1M LiPF$_6$ and (e) EIS/EMC 1M LiPF$_6$ electrolytes in Li$_{4+x}$Ti$_5$O$_{12}$/Li$_4$Ti$_5$O$_{12}$ symmetric cells. Mid-plateau polarization (ΔE) between delithiation and lithiation is indicated for the first cycle.

PCCP

ARTICLE

The sulfur containing species, formed by reduction of sulfones at the lithium electrode, are able to migrate toward the LTO electrode to be oxidized at a potential of 1.7 V vs. Li/Li$^+$ or 2.0 V vs Li/Li$^+$ as seen on the CVs reported in Figures 2 and 3, which can contribute to the formation of a resistive surface film that reduces the titanate electrode lifetime, regardless of what the cell configuration is.

Li$_{4+x}$Ti$_5$O$_{12}$/Li$_4$Ti$_5$O$_{12}$ symmetric cells

Symmetric Li$_{4+x}$Ti$_5$O$_{12}$/Li$_4$Ti$_5$O$_{12}$ cells have been constructed to unambiguously establish the failure mechanism of LTO half-cells in the presence of sulfones. In such cells, there is no quasi-infinite source of lithium as no metallic lithium is used. Furthermore, due to Li strong reducing nature, some parasitic reactions may occur at the lithium surface. These cannot take place in symmetric Li$_{4+x}$Ti$_5$O$_{12}$/Li$_4$Ti$_5$O$_{12}$ cells. Li$_4$Ti$_5$O$_{12}$ is lithiated to Li$_{4+x}$Ti$_5$O$_{12}$ (0 < x ≤ 3) at 1C rate in LTO/Li half-cells before being paired with a fresh Li$_4$Ti$_5$O$_{12}$ electrode. In the following experiments, the pre-lithiated Li$_7$Ti$_5$O$_{12}$ has, by construction, a lower capacity (Table 3) than the delithiated Li$_4$Ti$_5$O$_{12}$ electrode. In this configuration, the pre-lithiated Li$_7$Ti$_5$O$_{12}$ electrode acts as a limiting electrode in Li$_{4+x}$Ti$_5$O$_{12}$/Li$_4$Ti$_5$O$_{12}$ cells. During the galvanostatic tests, only flat plateaus (Figure 8) are observed for Li$_{4+x}$Ti$_5$O$_{12}$/Li$_4$Ti$_5$O$_{12}$ cells when using the ten electrolytes under study. The resulting capacities are higher for sulfones/EMC than EC/EMC but these values are in agreement with the capacities obtained at 1C rate in half-cells (Table 3). Also, the mid-plateau polarization at the first cycle (ΔE = 35 to 64 mV) is less important than in half-cells and remains constant over the cycling. Therefore, the huge polarization observed in half-cells is mainly due to electrochemical reactions occurring at the lithium electrode. In symmetric cells, ΔE is ranked as the reverse of the electrolyte conductivities following the order:
EC/EMC (8.83 mS cm^{-1}) < TMS/EMC (4.67 mS cm^{-1}) < EMS/EMC (4.36 mS cm^{-1})
< MIS/EMC (3.73 mS cm^{-1}) ≈ EIS/EMC (3.75 mS cm^{-1}).

Table 3 Pre-lithiation capacities of Li$_7$Ti$_5$O$_{12}$ electrodes obtained at the 1D rate in LTO/Li cells, before being incorporated in Li$_{4+x}$Ti$_5$O$_{12}$/Li$_4$Ti$_5$O$_{12}$ symmetric cells.

Sulfone-based electrolytes		Reference electrolytes	
	Q (mAh g^{-1})		Q (mAh g^{-1})
TMS/EMC (1/1)	152.0	EC/DMC (1/1)	126.3
TMS/DMC (1/1)	152.7	PC/DMC (1/1)	114.7
EMS/EMC (1/1)	150.8	EC/EMC (1/1)	117.1
EMS/DMC (1/1)	150.1	PC/EMC (1/1)	121.8
MIS/EMC (1/1)	149.6		
MIS/DMC (1/1)	150.0		
EIS/EMC (1/1)	146.6		
EIS/DMC (1/1)	149.6		

The same trend is noticeable when DMC is mixed with sulfone instead of EMC (Figure 9).

In the case of the reference EC/EMC highly conductive electrolyte, the cell polarization is mainly due to the resistivity of the electrolyte and Li$^+$ diffusion in the active material. Hence, this means that the influence of the Li$_x$Ti$_5$O$_{12}$ (4 ≤ x ≤ 7)/electrolyte interface impedances is low compared to that of the bulk electrolyte.

The surface films must be thin, porous and Li$^+$ conductive. Using symmetric cells, the coulombic efficiencies approach 100.0% as in the case of the reference electrolytes, no matter what the cycling rate is: values are comprised between 99.5% and 99.8% with either DMC or EMC as co-solvent (Figure S2). Capacity losses at C/5+D/5 rate are superior for sulfone-based electrolytes than the reference electrolytes, probably due to insufficient Li$^+$ transport in bulk electrolyte and across the two LTO/electrolyte interfaces. When alternating between slow and high cycling rates, the resulting capacities present the same behaviour over 100 cycles (Figure 10).
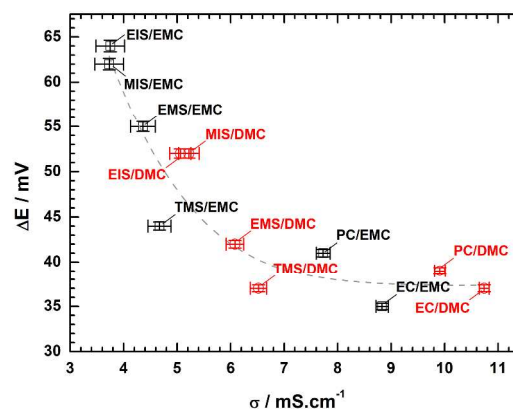
Fig. 9 Mid-plateau polarization (ΔE in mV) in Li$_{4+x}$Ti$_5$O$_{12}$/Li$_4$Ti$_5$O$_{12}$ cells as a function of both the nature and ionic conductivity of the electrolyte at 20.0 ± 0.3°C using LiPF$_6$ (1M) as salt.

PCCP

ARTICLE
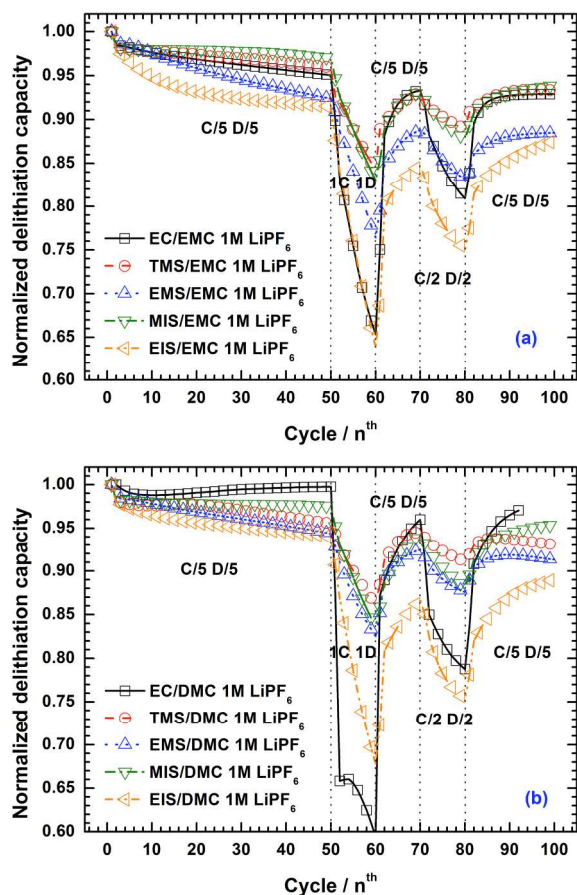
Fig. 10 Normalized delithiation capacity (Q/Q_0) at $20.0 \pm 0.3°C$ versus cycle number of $Li_{4+x}Ti_5O_{12}/Li_4Ti_5O_{12}$ cells for the five (a) EMC-based and (b) DMC-based electrolytes.

In the case of the highest rate, the losses are greater with the reference than with sulfone-based electrolytes in agreement with the pre-lithiation capacities (Table 3). Finally, reduced capacity losses and high coulombic efficiencies are observed when $Li_{4+x}Ti_5O_{12}/Li_4Ti_5O_{12}$ are used instead of Li half-cells, even if sulfones enter in the electrolyte composition. Among all tested sulfones, TMS and MIS mixed with EMC present as good performances as the reference EC/EMC electrolyte. Using DMC as co-solvent in binary mixtures, TMS and MIS give better performances, which remain nevertheless inferior to classical EC-based electrolytes.

Surface film characterization

SCANNING ELECTRON MICROSCOPY (SEM) Unlike EC/EMC, the EMS/EMC mixture is found to engender large capacity losses due to a great increase in resistivity at the electrode/electrolyte

interfaces (Figure 4 to Figure 7). These two solutions are thus chosen to be compared and exhibit major differences in the LTO/electrolyte interface morphology. Scanning electron microscopy is carried on titanate electrodes that have been cycled 100 times in LTO/Li half-cells. These electrodes are dried under vacuum at 50°C for 48 hours without being rinsed to avoid any passivation film dissolution in DMC.
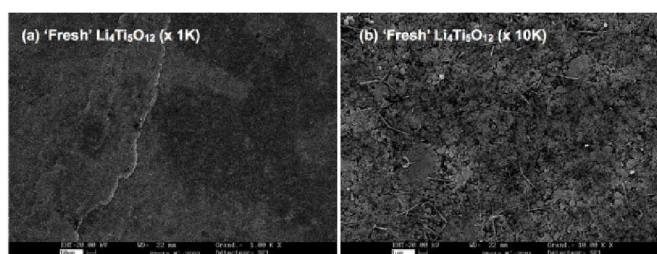
Fig. 11 SEM micrographs of the 'fresh' $Li_4Ti_5O_{12}$ electrode before cycling.
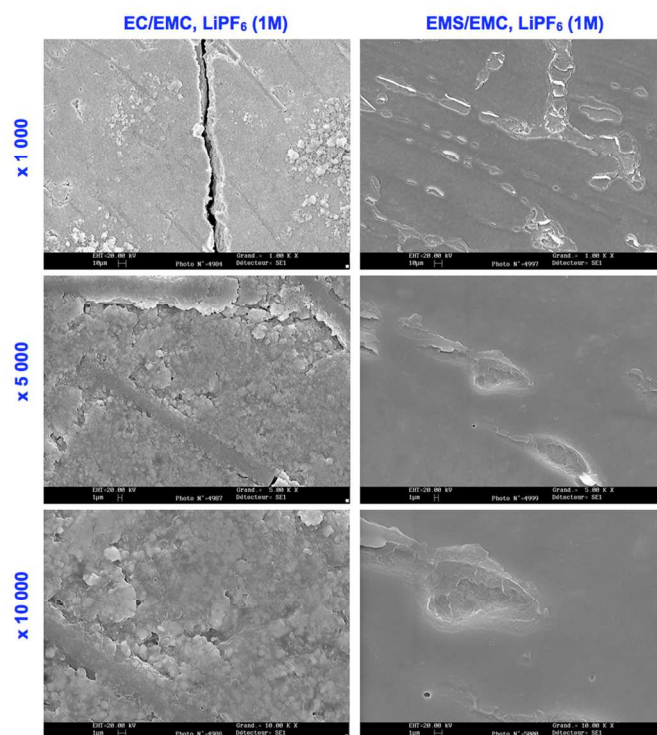
Fig. 12 SEM micrographs of $Li_7Ti_5O_{12}$ electrodes taken from $Li_4Ti_5O_{12}/Li$ half-cells after being cycled 100 times between 2.0 V vs. Li/Li^+ and 1.0 V vs. Li/Li^+ in EC/EMC +1M $LiPF_6$ and EMS/EMC +1M $LiPF_6$.

In Figure 11 are presented SEM micrographs for the 'fresh' (non-cycled) LTO electrode. Small particles of $Li_4Ti_5O_{12}$ active material mixed, which carbon black and PVdF can be observed. In the case of cycled LTO electrodes (Figure 12), surface

modifications are easily visible. The EC/EMC electrolyte is responsible for a thin passivation film formation. In the EMS/EMC mixture, huge amounts of organic material are observed at the electrode surface after 100 cycles, resulting in an increase of half-cell polarization and resistivity (Figure 4, Figure 6, Figure 7). The resulting SEI is not still suitable for facilitating the Li$^+$ insertion/extraction.

In the symmetric configuration of the cells, the resulting surface films should be too thin to be detected by SEM, because of a lower interface resistivity compared to LTO/Li coin-cells (Figure 9).

XPS Sulfone-based electrolytes TMS/EMC and EMS/EMC (LiPF$_6$, 1M) are responsible for large capacity losses in Li$_4$Ti$_5$O$_{12}$/Li half-cells that are accompanied by an impedance increase of the accumulators. The EC/EMC electrolyte ensures the lowest capacity loss and a better reversibility during cycling, as compared to other EMC-based electrolytes. The aim of this XPS study is thus to identify surface species deposited on the titanate electrode causing capacity losses when TMS and EMS are used in Li$_4$Ti$_5$O$_{12}$/Li cells, by examining high resolution spectra from Li 1s, F 1s, P 2p, C 1s, S 2p, and Ti 2p core orbitals.

Li 1s, F 1s and P 2p XPS spectra of Li$_7$Ti$_5$O$_{12}$ electrodes cycled 100 times in Li$_4$Ti$_5$O$_{12}$/Li accumulators are presented in Figure 13. Li 1s and F 1s spectra reveal important amounts of LiF at the electrode surface (from 25 at. % to 30 at. %). P 2p spectra show that the Li$_x$PF$_y$ and Li$_x$PF$_y$O$_z$ species are present in close relative quantities for the three EMC-based electrolytes. The C 1s spectra shown in Figure 14 reveal a SEI formation coming essentially from alkylcarbonate decomposition products (EMC) on the Li$_7$Ti$_5$O$_{12}$ surface, including the C-C/C-H, C-O and O-C=O bonds. Their abundance is presented in Table 4.

Table 4 C 1s XPS spectra peak attribution and their abundance at the Li$_7$Ti$_5$O$_{12}$ electrode surface.

		Li$_4$Ti$_5$O$_{12}$/Li cells		
	Binding energy (eV)	Electrolytes (LiPF$_6$, 1M)		
		EC/EMC	EMS/EMC	TMS/EMC
C	283.4	0	0	4.1
C-C/C-H	285	42.2	57.1	45.4
C-O	286.9 ± 0.1	44.7	31.1	35.6
C=O/O-C=O	289.2 ± 0.2	9.7	9.2	7.4
CO$_3$	290.1 ± 0.2	3.4	2.3	7.5

The relative contribution of the carbon in the C 1s spectrum is different, depending on the choice of the electrolyte. In the absence of sulfones (i.e. EC/EMC), a greater contribution of the oxidized carbons (C-O peak at 287 eV) is observed because of both the EC and the EMC contribution to the formation of the electrode/electrolyte interface (Figure 14). Concerning the sulfone electrolytes, carbon black from the composite electrode is detected on the surface when TMS/EMC is used, indicating

that the surface layer is thinner compared to EMS/EMC. This confirms the impedance results presented in Figure 6 and Figure 7.
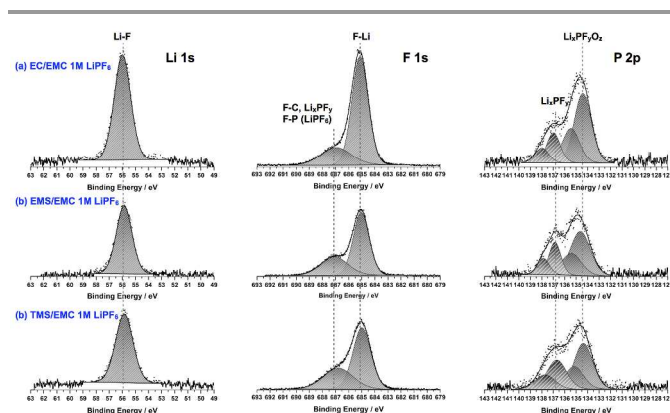
Fig. 13 Li 1s, F 1s, P 2p XPS spectra of Li$_7$Ti$_5$O$_{12}$ electrodes cycled 100 times in Li$_4$Ti$_5$O$_{12}$/Li cells using the (a) EC/EMC, (b) EMS/EMC and (c) TMS/EMC (LiPF$_6$, 1M) electrolytes.
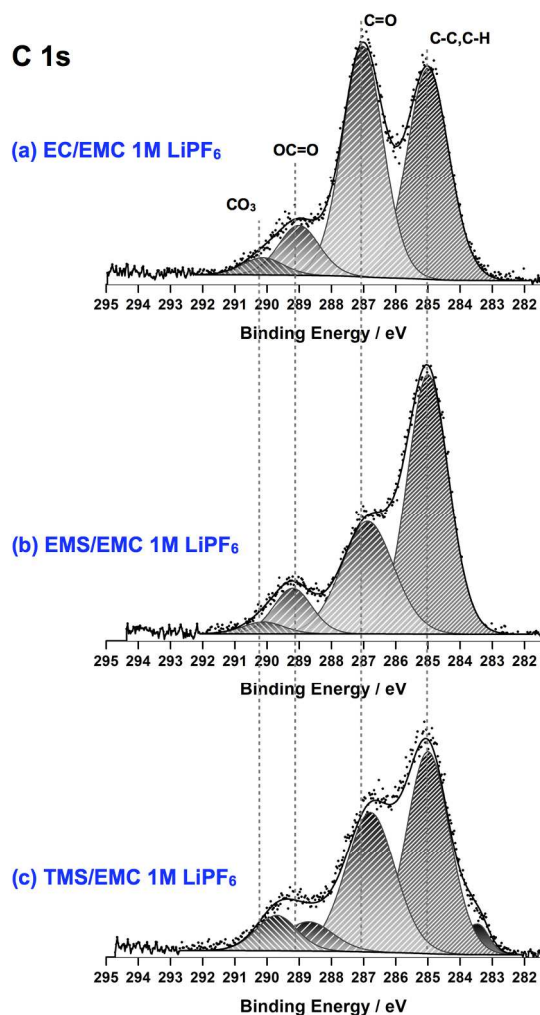
Fig. 14 C 1s XPS spectra of Li$_7$Ti$_5$O$_{12}$ electrodes cycled 100 times in LTO/Li half-cells using the (a) EC/EMC, (b) EMS/EMC and (c) TMS/EMC (LiPF$_6$, 1M) electrolytes.

(a) EC/EMC 1M LiPF$_6$

S-O (RSO$_2^-$)
S-O (RSO$_3^-$)
S 2p
S-S (RS*SO$_x$R, RS*SO$_3^-$) or TMS

(b) EMS/EMC 1M LiPF$_6$

(c) TMS/EMC 1M LiPF$_6$
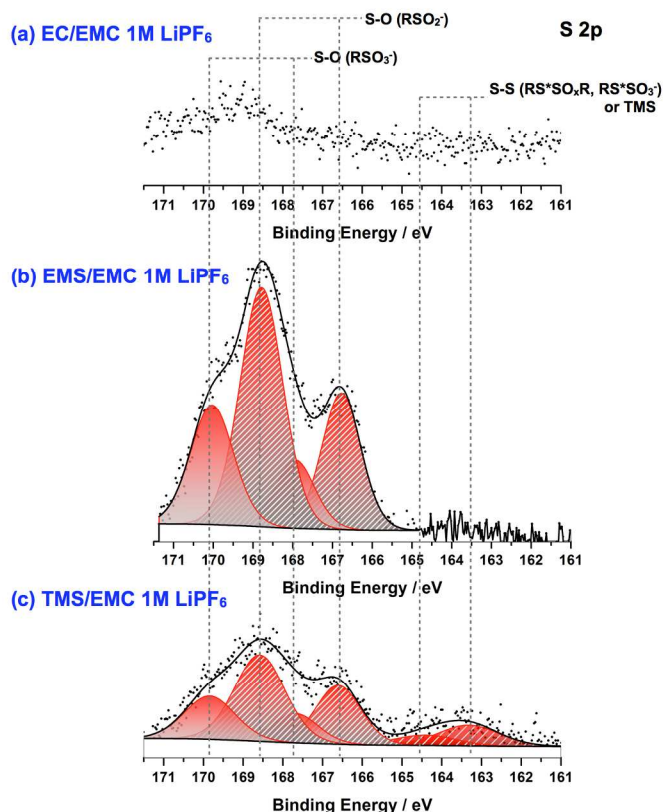
Fig. 15 S 2p XPS spectra of Li$_7$Ti$_5$O$_{12}$ electrodes cycled 100 times in Li$_4$Ti$_5$O$_{12}$/Li half-cells using the (a) EC/EMC, (b) EMS/EMC and (c) TMS/EMC (LiPF$_6$, 1M) electrolytes.

Nevertheless, titanium is not detected at the electrode surface for the three EMC-based electrolytes, most likely due to the heterogeneity of the SEI, which may form specifically on the active material.[15] In order to know about the chemical composition of sulfone degradation products at the LTO surface, the S 2p XPS spectra are presented on Figure 15 for the three electrodes previously analysed. RSO$_2^-$, RSO$_3^-$ species are detected on the electrode surface when sulfones are utilized in the electrolytes.[16,17] These two species are formed following reactions (1) and (2):

(1) $RSO_2R + Li^+ + e^- \rightarrow RSO_2Li + R^\bullet$; $R^\bullet + e^- + H^+ \rightarrow RH$ [18]

(2) $2RSO_2^- \rightarrow RSO_3^- + RSO^-$
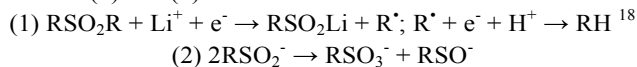
In the case of the TMS/EMC electrolyte, peaks around 164 eV are detected. They may be attributed to either TMS or other compounds, such as RSSO$_x$R (Figure 15c). Li *et al.* show that the reduction of TMS at the surface of graphite leads to the formation of Li$_2$SO$_3$ and RSO$_3$Li after 1 cycle.[19] Furthermore, if the peak at 164 eV corresponds to alkylsulfurs (RSR'), they could be formed according to reaction 3:

(3) $RSO_2R' + 4e^- + 4Li^+ \rightarrow Li_2O + RSR'$ [20,21]
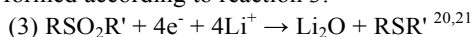
RSR' species are able to migrate toward the LTO electrode in lithium cells to be oxidized into disulfur or polysulfur (RSSR', S$_x^{n-}$, etc…). This is the reason why sulfinates, sulfonates and probably coloured disulfur are found at the LTO surface (Figure 15).

Both electrodes Li$_7$Ti$_5$O$_{12}$ and Li$_{4+x}$Ti$_5$O$_{12}$ coming from symmetric cells were cycled 100 times in EC/EMC and EMS/EMC electrolytes before being retrieved and dried under vacuum for 48 hours at 50°C. The choice of these electrolytes aims to exhibit major differences in the interface chemistry, in relation with the contrast in electrochemical performances of symmetric cells (Figure 8 and Figure 10). These cells allow not only to study a single interface of identical chemical nature: Li$_{4+x}$Ti$_5$O$_{12}$/electrolyte; but also to get information from the surface composition at different states of charge of the LTO electrode. This allows knowing the dynamics of the electrode/electrolyte interface during cycling.

In Figure 16 are presented the C 1s spectra obtained for both the working electrode (Li$_7$Ti$_5$O$_{12}$) and the counter-electrode (Li$_{4+x}$Ti$_5$O$_{12}$) taken from symmetric cells. A very thin layer is found on the counter-electrode. Carbon black (C 1s) is clearly visible around 283.5 eV on the oxidized (counter) electrode. Concerning the working (reduced) electrode, the carbon black signal is only visible in the case of the EMS/EMC mixture. Also, the S 2p spectra show that no sulfur species is deposited on the electrodes after being cycled in the EMS/EMC electrolyte. Therefore, the passivation layer formation on the Li$_4$Ti$_5$O$_{12}$ electrode is provided by the EMC reactivity in this binary electrolyte. Hence, EMS does not contribute to the formation of an organic layer at the LTO/electrolyte interface. When EC/EMC is used, both the EC and the EMC contribute to the organic layer formation. This results in the formation of covering surface films due to polymer formation instead of oligomers formed with the single carbonate mixture EMS/EMC. This lowers carbon black C 1s peak intensity for the working electrode.

Large amounts of LiF (30 at. % to 35 at.%) are found on both the working and the counter-electrode after cycling in symmetric cells (Figure 17). As this compound is partially or readily soluble in the electrolyte,[22] LiF may be found on both electrodes even if it is formed on the active material of the composite electrode.[23] The lower peak intensities found for EC/EMC confirm that the surface layer is thicker than the one formed using the EMS/EMC electrolyte. Other compounds coming from the EMC reduction (ROCO$_2$Li and Li$_2$CO$_3$) are also detected on the electrode surface when the EMS/EMC electrolyte is used.

PCCP

ARTICLE

C 1s
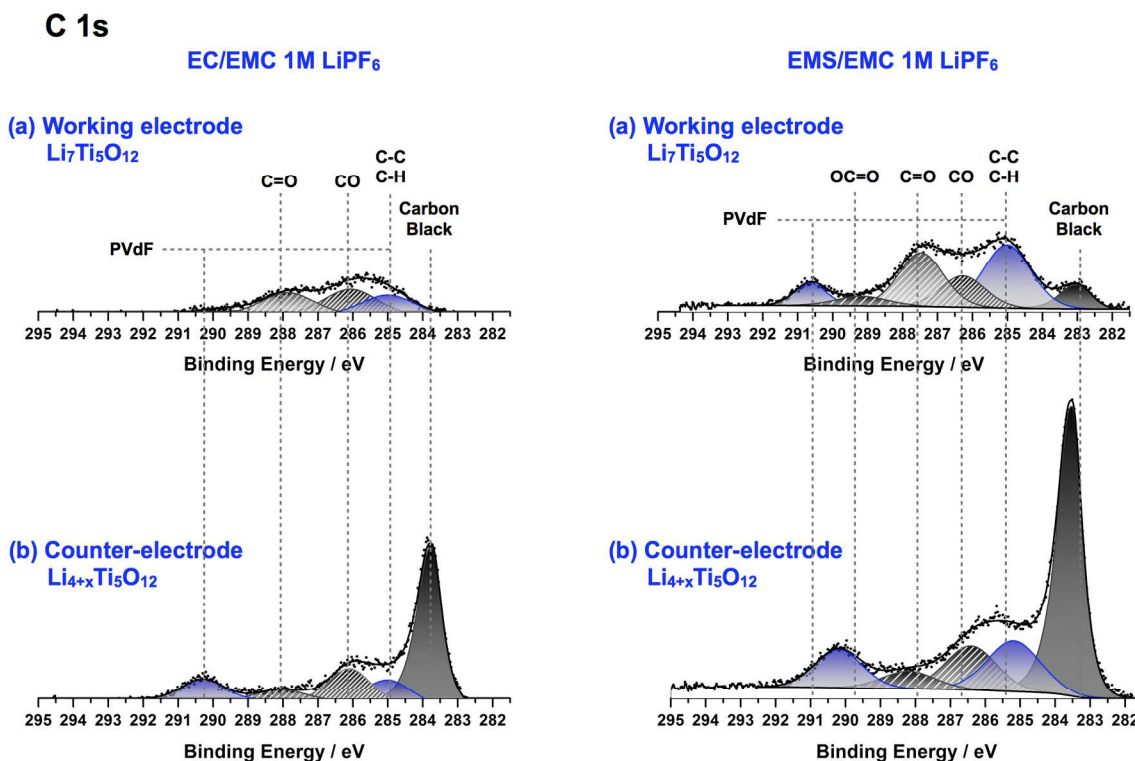
Fig. 16 C 1s spectra of (a) $Li_7Ti_5O_{12}$ and (b) $Li_{4+x}Ti_5O_{12}$ electrodes cycled 100 times in $Li_{4+x}Ti_5O_{12}/Li_4Ti_5O_{12}$ symmetric cells using the (on the left) EC/EMC and (on the right) EMS/EMC electrolytes ($LiPF_6$, 1M).
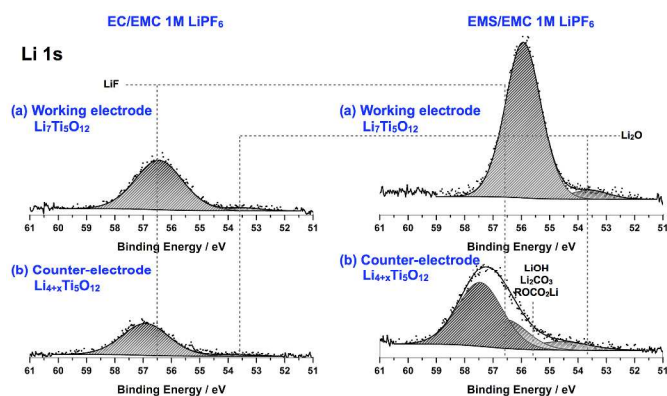
Fig. 17 Li 1s spectra of (a) $Li_7Ti_5O_{12}$ and (b) $Li_{4+x}Ti_5O_{12}$ electrodes cycled 100 times in $Li_{4+x}Ti_5O_{12}/Li_4Ti_5O_{12}$ symmetric cells using the (on the left) EC/EMC and (on the right) EMS/EMC electrolytes ($LiPF_6$, 1M).

Conclusions

Sulfones are an alternative to cyclic carbonates as component of an electrolyte for Li-ion batteries working at high voltage such as $LiNi_xMn_{2-x}O_4$/LTO cells. Potentiostatic and galvanostatic tests using LTO/Li half-cells confirm the excellent cycleability and reversibility of the LTO electrode in EC/DMC and EC/EMC electrolytes containing $LiPF_6$ (1M). However, when EC is replaced by sulfones, parasitic reactions occur at the Li interface leading to a bad cycleability of LTO/Li cells. Reduced species, which are soluble in the electrolytes, are able to migrate toward the positive $Li_4Ti_5O_{12}$ electrode to be deposited in the form of resistive interphases. This causes large capacity losses of the LTO electrode and the failure of the $Li_4Ti_5O_{12}$/Li cells.

In order to study the $Li_4Ti_5O_{12}$/electrolyte interface without any interference coming from the negative electrode, $Li_{4+x}Ti_5O_{12}/Li_4Ti_5O_{12}$ symmetric cells were built and then cycled. In sulfone-based electrolytes, the LTO can be satisfactorily cycled. EIS measurements reveal that the two $Li_{4+x}Ti_5O_{12}$/electrolyte interfaces ($0<x<3$) exhibit a low resistivity, to the point that a correlation between the bulk electrolyte ionic conductivity of the cell polarization could be found. XPS surface analysis of the two LTO interfaces, one partially oxidized and one reduced, taken from a symmetric cell, indicates that sulfones do not participate in the formation

of the surface layers. Alkylcarbonates (EMC or DMC), used as co-solvents in sulfone-based binary electrolytes, ensure the formation of the LTO surface layers. In EC/EMC reference electrolyte, the two alkylcarbonates (EC and EMC) contribute to the surface layer formation resulting in covering surface films, as compared to EMS/EMC. It has also been found that the film covering effect depends on the state of charge of the LTO electrode: the deposits must be thinner on the oxidized electrode than on the reduced electrode. Therefore, the deposit occurs mainly during the reduction step and partial dissolution during the oxidation.

Among tested sulfones, MIS (methyl isopropyl sulfone) and TMS (tetra methyl sulfone) provide the best performances at the LTO electrode, but owing to a more pronounced fading they remain inferior to those obtained using the EC/DMC reference electrolyte (LiPF$_6$, 1M).

Acknowledgements

Notes and references

[a] CEA/DAM, Le Ripault, F-37260, Monts, France.

[b] Laboratoire de Recherche Correspondant, LRC CEA/LPCM2E n°1, France.

[c] Université François Rabelais, Laboratoire de Physico-Chimie des Matériaux et des Electrolytes pour l'Energie (LPCM2E), Parc de Grandmont, F-37200, Tours, France.

[d] CEA/DRT/LITEN, Minatec Campus, F-38000, Grenoble, France

[e] Present address at: Chemistry Department, University of Rhode Island, Kingston, RI 02881, USA. Email: jdemeaux@chm.uri.edu.

1.   J. M. Tarascon and M. Armand, *Nature*, 2001, **414**, 359-367.

2.   M. Armand and J. M. Tarascon, *Nature*, 2008, **451**, 652-657.

3.   S. Patoux, L. Sannier, H. Lignier, Y. Reynier, C. Bourbon, S. Jouanneau, F. Lecras and S. Martinet, *Electrochimica Acta*, 2008, **53**, 4137-4145.

4.   X.-G. Sun and C. A. Angell, *Electrochemistry Communications*, 2005, **7**, 261-266.

5.   A. Abouimrane, I. Belharouak and K. Amine, *Electrochemistry Communications*, 2009, **11**, 1073-1076.

6.   J. C. Burns, L. J. Krause, D.-B. Le, L. D. Jensen, A. J. Smith, D. Xiong and J. R. Dahn, *Journal of The Electrochemical Society*, 2011, **158**, A1417.

7.   R. Oesten, U. Heider and M. Schmidt, *Solid State Ionics*, 2002, **148**, 391-397.

8.   L. J. Krause, L. D. Jensen and J. R. Dahn, *Journal of The Electrochemical Society*, 2012, **159**, A937-A943.

9.   K. Nakura, Y. Ohsugi, M. Imazaki, K. Ariyoshi and T. Ohzuku, *Journal of The Electrochemical Society*, 2011, **158**, A1243.

10.   K. Xu and C. A. Angell, *Journal of The Electrochemical Society*, 2002, **149**, A920.

11.   K. Xu and C. A. Angell, *Journal of The Electrochemical Society*, 2002, **149**, L7.

12.   S. Chellammal, M. Noel and P. N. Anantharaman, *Journal of the Chemical Society, Perkin Transactions 2*, 1993, **0**, 993-997.

13.   G.-N. Zhu, Y.-G. Wang and Y.-Y. Xia, *Energy & Environmental Science*, 2012, **5**, 6652-6667.

14.   M. G. S. R. Thomas, P. G. Bruce and J. B. Goodenough, *Journal of The Electrochemical Society*, 1985, **132**, 1521-1528.

15.   Y.-B. He, B. Li, M. Liu, C. Zhang, W. Lv, C. Yang, J. Li, H. Du, B. Zhang, Q.-H. Yang, J.-K. Kim and F. Kang, *Scientific Reports*, 2012, **2**.

16.   Y. Diao, K. Xie, S. Xiong and X. Hong, *Journal of The Electrochemical Society*, 2012, **159**, A1816-A1821.

17.   R. Holm, in *Department of Applied Physics, Bayer AG*, Leverkusen, pp. 37-72.

18.   K. Chiba, T. Ueda, Y. Yamaguchi, Y. Oki, F. Shimodate and K. Naoi, *Journal of The Electrochemical Society*, 2011, **158**, A872.

19.   S. Li, X. Xu, X. Shi, B. Li, Y. Zhao, H. Zhang, Y. Li, W. Zhao, X. Cui and L. Mao, *Journal of Power Sources*, 2012, **217**, 503-508.

20.   J. N. Gardner, S. Kaiser, A. Krubiner and H. Lucas, *Can. J. Chem.*, 1973, **51**, 1419-1421.

21.   E. Akgun, K. Mahmood and C. A. Mathis, *J. Chem. Soc., Chem. Commun.*, 1994, **0**, 761-762.

22.   L. Castro, R. Dedryvère, J. B. Ledeuil, J. Bréger, C. Tessier and D. Gonbeau, *Journal of The Electrochemical Society*, 2012, **159**, A357.

23.   K. Edström, T. Gustafsson and J. O. Thomas, *Electrochimica Acta*, 2004, **50**, 397-403.

Physical Chemistry Chemical Physics Accepted Manuscript
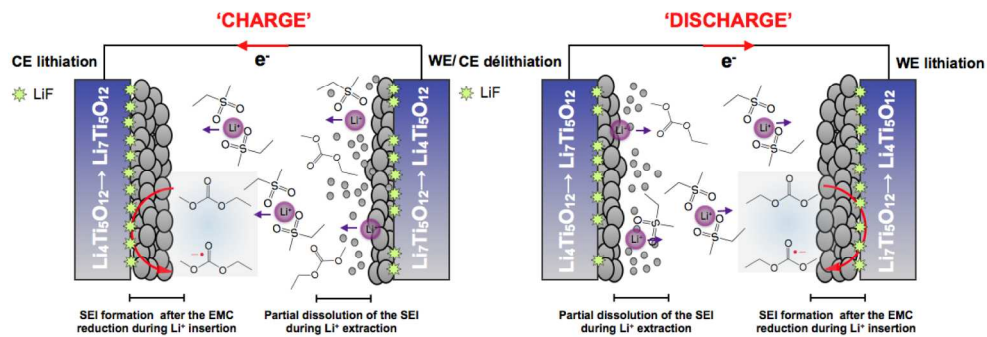
Dynamics of the two LTO/sulfone-mixed electrolyte interfaces in a LTO/LTO symmetric cell.
880x300mm (72 x 72 DPI)